HHS Public Access

Author manuscript

J Neural Eng. Author manuscript; available in PMC 2019 February 01.

Published in final edited form as:

J Neural Eng. 2018 February 01; 15(1): 016020–. doi:10.1088/1741-2552/aa976a.

Overexpression of cypin alters dendrite morphology, single neuron activity, and network properties via distinct mechanisms

Ana R. Rodríguez[1,2], **Kate M. O'Neill**[1,2], **Przemyslaw Swiatkowski**[1,3], **Mihir V. Patel**[1,4], and **Bonnie L. Firestein**[1,3]

[1]Department of Cell Biology and Neuroscience, Rutgers University, 604 Allison Road, Piscataway, NJ, 08854, USA

[2]Graduate Program in Biomedical Engineering, Rutgers University, 599 Taylor Road, Piscataway, NJ, 08854, USA

[3]Graduate Program in Cellular and Molecular Pharmacology, Molecular Biosciences, Rutgers University, 604 Allison Road, Piscataway, NJ, 08854, USA

[4]Graduate Program in Neuroscience, Rutgers University, 604 Allison Road, Piscataway, NJ, 08854, USA

[5]Graduate Faculty in Biomedical Engineering, Rutgers University, 599 Taylor Road, Piscataway, NJ, 08854, USA

Abstract

Objective—This study investigates the effect that overexpression of **cy**tosolic **P**SD-95 **in**teractor (cypin), a regulator of synaptic PSD-95 protein localization and a core regulator of dendrite branching, exerts on the electrical activity of rat hippocampal neurons and networks.

Approach—We cultured rat hippocampal neurons and used lipid-mediated transfection and lentiviral gene transfer to achieve high levels of cypin or cypin mutant (cypinΔPDZ; PSD-95 non-binding) expression cellularly and network-wide, respectively.

Main results—Our analysis revealed that although overexpression of cypin and cypinΔPDZ increase dendrite numbers and decrease spine density, cypin and cypinΔPDZ distinctly regulate neuronal activity. At the single cell level, cypin promotes decreases in bursting activity while cypinΔPDZ reduces sEPSC frequency and further decreases bursting compared to cypin. At the network level, by using the Fano factor as a measure of spike count variability, cypin overexpression results in an increase in variability of spike count, and this effect is abolished when cypin cannot bind PSD-95. This variability is also dependent on baseline activity levels and on mean spike rate over time. Finally, our spike sorting data show that overexpression of cypin results in a more complex distribution of spike waveforms and that binding to PSD-95 is essential for this complexity.

Significance—Our data suggest that dendrite morphology does not play a major role in cypin action on electrical activity.

Correspondence: Bonnie L. Firestein, Ph.D., Department of Cell Biology and Neuroscience, Rutgers University, 604 Allison Road, Piscataway, NJ, 08854, USA; Phone: 848-445-8045; firestein@biology.rutgers.edu.

Keywords

neuronal networks; Fano factor; spike sorting; hippocampal neurons; cytosolic PSD-95 interactor (cypin); dendrites; electrophysiology

Introduction

Proper synaptic transmission is essential for normal brain function and requires the precise spatial and functional assembly of molecular signal transduction machinery at synaptic sites and the correct morphology of dendrites and their branches [1]. The postsynaptic density (PSD), an electron-dense region that characterizes the membranes of postsynaptic neurons, is a dynamic and complex structure. The composition of the PSD has been widely studied, and it has been proposed that the PSD serves as a network composed of scaffolding and cytoskeletal proteins that localize signaling molecules, receptors, and ion channels at the synapse [2]. Therefore, the organization of these proteins is critical for the regulation of synaptic transmission and synaptic plasticity. Moreover, defects in dendritogenesis and synaptogenesis contribute to neurological and neurodevelopmental disorders [3].

PSD-95 is a member of the membrane-associated guanylate kinase (MAGUK) family of proteins and is found at the PSD of excitatory glutamatergic synapses [4], where it has been associated with the trafficking and anchoring of all three classes of glutamate receptors – kainate, alpha-amino-3-hydroxy-5-methyl-4-isoxazolepropionic acid (AMPA), and N-methyl-D-aspartate (NMDA) type glutamate receptors. Cypin (**cy**tosolic **P**SD-95 **in**teractor) was originally identified as a highly abundant PSD-95-binding protein in brain extracts [5]. Overexpression of cypin in rat hippocampal cultures disturbs postsynaptic localization of PSD-95 and SAP102 (**s**ynapse **a**ssociated **p**rotein 102), a related neuronal MAGUK protein [5]. In mature hippocampal cultures, both PSD-95 and SAP102 are targeted and clustered in dendrites at discrete spots that are likely to reflect postsynaptic sites. When cypin is overexpressed in culture, a significant reduction of PSD-95 and SAP102 clusters is observed. Immunostaining for the presynaptic marker synaptophysin demonstrates that the total number of synaptic sites is not altered and that cypin specifically regulates the synaptic targeting of associated MAGUK proteins [5].

Numerous studies show that changes in PSD-95 expression drive the maturation of dendritic spines and influence synaptic targeting and trafficking of glutamate receptors, resulting in alterations in the electrical activity of glutamatergic synapses [4, 6-10]. Overexpression of PSD-95 in hippocampal slice cultures specifically recruits AMPA receptors (AMPARs) to synapses and enhances AMPAR-mediated excitatory postsynaptic currents (EPSCs) with no change in NMDAR-mediated EPSCs [11]. Moreover, impaired AMPAR function occurs in PSD-95 knockout mice [8]. This disruption in activity is specifically due to the fact that a significant proportion of synapses lack functional AMPARs, independent of spine morphology, supporting the need to understand both the structural and functional implications of altering levels of PSD-95 and its interactors in hippocampal neurons.

Here, we analyze the effects of cypin or a mutant of cypin that cannot bind to PSD-95 (cypinΔPDZ) on dendrite morphology, spine number, and single cell electrophysiology. We

also use microelectrode arrays (MEAs) to record the activity of networks of hippocampal neurons that overexpress cypin or cypinΔPDZ, and we report the first use of lentiviral gene transfer for global overexpression of proteins in high density neuronal cultures on MEAs. We analyze changes in the electrical activity of our networks 7 and 11 days after lentiviral transduction and find that the initial activity level of a network influences its long term activity. Furthermore, we quantify the variability of the spike count of the networks and find that spiking variability increases after cypin overexpression in a PSD-95-binding-dependent manner. Our data demonstrate that only networks that overexpress cypin, but not cypinΔPDZ, show significant changes in the correlation between spike count variability and spike rate. Finally, we perform spike sorting and show that networks that overexpress cypin exhibit a more robust spike type composition over time that can potentially be attributed to an enhanced dendritic arbor. However, we find that overexpression of cypin or cypinΔPDZ increases dendrites in a similar manner, suggesting that all of the network changes that are promoted by cypin are not solely due to increased dendrites. Taken together, our data suggest that cypin alters single cell electrophysiology and network dynamics independent of its role in PSD-95 localization.

Materials and Methods

Cell culture

Neuronal cultures were prepared from hippocampi of rat embryos at 18 days of gestation (E18) [5]. After isolation, meninges were removed and the hippocampi were mechanically dissociated by pipetting through the bore of a fire-polished Pasteur pipette. Prior to plating, MEAs (Multi Channel Systems, Germany) were coated with 0.5 mg/ml poly-D-lysine (Sigma) for at least 1 hour, washed three times with sterile water, and coated with 10 μg/ml laminin (Sigma) for at least 30 minutes. Cells were plated onto MEAs at a density of 1×10^6 cells/MEA. Cultures were maintained in NbActiv4 medium (BrainBits, LLC) at 37 °C and 5% CO2. Half medium changes were performed every other day. Cells were plated at a density of 200,000 cells/well in 24 well plate for dendrite branching studies and single cell electrophysiology experiments and at a density of 100,000 cells/well in 24 well plate for spine analysis. All animals were cared for ethically in accordance with Institutional Animal Care and Use Committee (IACUC) standards.

Lentiviral particle production and transduction

The lentiviral plasmids were constructed by subcloning cDNA encoding wild type cypin or cypinΔPDZ into the control FG12 vector containing EGFP for expression (vector was a gift from Dr. Chris Pröschel, University of Rochester School of Medicine). Lentiviral particles were generated by transfecting HEK293TN cells (ATCC) using the calcium phosphate precipitation method with one of the lentiviral plasmids, the packaging plasmid psPAX2, and the envelope plasmid pMD2.G (VSV-G). The medium was replaced 24 hours post-transfection, and the medium containing viral particles was collected 48 hours later, concentrated using PEG-it virus precipitation solution (System Biosciences) according to the manufacturer's instructions, and stored at -80 °C until use. HEK293TN cells were maintained and transfected in Dulbecco's Modified Eagle Medium (DMEM; Gibco) supplemented with 10% fetal bovine serum (Atlanta Biologicals). Neuronal cultures were

transduced with lentiviral supernatant on day *in vitro* (DIV) 10. Half of the culture medium was changed 36 hours later and every other day from then on. Successful transduction was confirmed through fluorescence microscopy (Figure 1(A) and (B)).

Assessment of Dendritic Spine Number

Cultured hippocampal neurons were co-transfected on DIV14 with RFP and GFP, GFP-cypin, or GFP-cypinΔPDZ, using the calcium phosphate method. Neurons were fixed on DIV17 and immunostained for GFP and RFP. Images of dendritic segments were taken with a 60x plan apochromat oil immersion objective (NA 1.4) using a Yokogawa CSU-10 spinning disk confocal head attached to an inverted fluorescence microscope (Olympus IX50). X-, Y-, and Z-resolutions were set as 0.067 μm, 0.067 μm and 0.1 μm, respectively, to define dendritic spines. Spines were counted along dendritic segments starting from 20 μm to 80 μm from the soma. For each cell, segments were quantified and averaged. Spines were manually counted from at least 13 neurons for each experimental condition, and analysis was performed with the experimenter blinded to the condition. Statistics were calculated by one-way ANOVA followed by Tukey's multiple comparisons test.

Assessment of Dendrite Number

Cultured hippocampal neurons were transfected on DIV7 using Lipofectamine LTX with Plus reagent (Invitrogen) according to the manufacturer's instructions. Neurons were fixed on DIV12 with 4% paraformaldehyde in PBS for 15 minutes, washed 3 times with PBS, and then incubated in blocking solution (2% normal goat serum, 0.1% Triton X-100, and 0.02% sodium azide in PBS) for 1 hour. All antibodies used were diluted in blocking solution. Neurons were incubated for 1 hour at room temperature or overnight at 4 °C with primary antibodies: GFP (DSHB-12A6) was used to identify transfected cells, and MAP2 (BD Biosciences) was used to identify neurons. They were then washed with PBS 3 times and incubated for 1 hour at room temperature with appropriate secondary antibodies. Coverslips were mounted onto glass slides with Fluoromount-G (Southern Biotechnology). Transfected cells were visualized by immunofluorescence on an EVOS FL microscope at 20X (Thermo Fisher Scientific).

Semi-automated Sholl analysis was performed as described previously [12-15]. Briefly, images of hippocampal neurons were traced using the NeuronJ plugin for ImageJ (NIH). The tracing files were converted to SWC files using MATLAB (Mathworks) for further manipulation. NeuronStudio was then used to define the connectivity pattern between the segments, and the morphological data were exported to Excel using MATLAB. The experimenter was blinded to the condition when performing dendrite analysis. The axon was excluded based on MAP2 immunostaining absence.

Statistics were calculated by two-way ANOVA followed by Bonferroni multiple comparisons test.

Single cell recordings

Whole cell patch-clamp recordings were obtained from the soma of hippocampal neurons as described previously [16]. Recordings were performed on DIV21. The external solution

contained the following (in mM): 140 NaCl, 5 KCl, 2 CaCl2, 2 MgCl2, 10 HEPES, and 10 glucose (pH 7.4 adjusted with NaOH; 290–310 mOsmol). Recording electrodes (3–5 MΩ) contained a K^+-based internal solution composed of the following (in mM): 126 K-gluconate, 4 KCl, 10 HEPES, 4 ATP-Mg, 0.3 GTP-Na2, and 10 phosphocreatine (pH 7.2; 280–300 mOsmol). The membrane potential was held at –70 mV throughout all experiments. Data were amplified and filtered at 2 kHz by a patch-clamp amplifier (Multiclamp 700B), digitalized (DIGIDATA 1440A), stored, and analyzed by pCLAMP (Molecular Devices). Data were discarded when the input resistance changed >20% during recording. Statistics were calculated by one-way ANOVA followed by Tukey's multiple comparisons test.

MEA Recordings

Standard MEAs containing 60 planar electrodes (59 recording electrodes and 1 internal reference electrode), each with a 10 μm diameter and an interelectrode spacing of 200 μm (60MEA200/10iR-Ti-gr; Multi Channel Systems, Germany), were used for all experiments. Baseline recordings were performed on DIV10 immediately before lentiviral transduction and subsequently on DIV17 and DIV21. Prior to each recording, the culture medium was saved and replaced with recording solution (144 mM NaCl, 10 mM KCl, 1 mM MgCl2, 2 mM CaCl2, 10 mM HEPES, 2 mM Na-pyruvate, 10 mM glucose, pH 7.4), and the MEA was placed in the cell culture incubator for 5 minutes to allow the culture to reach equilibrium. After each recording, the cultures were washed twice with fresh culture medium before adding the saved conditioned medium. Each MEA was covered with a semipermeable lid (ALA MEA-MEM; ALA Scientific) during handling and recordings to prevent contamination from airborne pathogens. Spontaneous electrical signals were monitored and recorded for 5 minutes using the data acquisition commercial software MC_Rack (Multi Channel Systems) as described previously by our group [17, 18]. The temperature of the cultures was maintained at 37 °C on a heat-controlled stage during recordings, and the signals were sampled at 20kHz with an MEA1060-Inv-BC amplifier (Multi Channel Systems).

Neuronal networks naturally go through periods of inactivity while in regular growth medium. Therefore, to ensure that the observed changes in network activity are indeed due to exogenous protein expression and not due to the networks being in a different “state”, it is necessary to use recording medium to regularize spiking and bursting. This was explored and tested in our previously published studies [17, 18]. Moreover, controls were run in these previously published works to show that this is an appropriate amount of time for networks to equilibrate. Importantly, networks cannot survive long-term in recording medium because the only source of nutrients is a small amount of glucose. Previous data from our laboratory show that the number of electrodes that remain electively active do not change over time, suggesting that neurons survive on the MEAs [17].

Signal Processing

The raw data were imported into MATLAB (MathWorks, Inc.) using MEA-Tools, an open-source toolbox. The signals were filtered through a fourth order Butterworth filter (20-2,000Hz) and a notch filter to remove the 60Hz electric hum. The electrodes that

exhibited irregular activity or excessive noise were excluded from the analysis. Spikes were detected using an adaptive threshold. Briefly, a spike was defined as a signal with voltage exceeding a positive or negative threshold, chosen to be 4.5 standard deviations times the background noise for every 10s window for each recording channel. Spikes were detected at their maximum absolute value, and interspike intervals had to be ≥ 2ms to prevent detecting the same spike twice.

Fano factor analysis

The spike count Fano factor of the neuronal networks was calculated as a measurement of spiking variability. The Fano factor is defined as the ratio of the variance to the mean of the spike count in a given time interval [19]. For every 300s recording, we calculated a Fano factor every 10 seconds and averaged all Fano factor to obtain the mean Fano factor of the entire network. For a random process with a Poisson distribution, the Fano factor is theoretically 1 due to the variance and the mean being equal [19, 20]. In contrast, regular spike rates exhibit a Fano factor that trends towards 0, and high Fano factors are characteristic of irregular spiking [21, 22]. Statistics were calculated by one-way ANOVA followed by Tukey's multiple comparisons test.

Spike Sorting

We applied Wave clus, a spike sorting algorithm, to obtain information about individual neurons within our networks [23]. Spike sorting extracts features from each spike and clusters them in classes that best reflect their shape. Wave clus calculates the wavelet transform for each spike and uses a set of the obtained wavelet coefficients as input for a clustering algorithm based on k-nearest neighbor interactions. Using the wavelet transform instead of principal component analysis (PCA) to extract the shape information allows for more specific discerning of spike features [23, 24]. We first detected individual spikes as described above. For each detected spike, we collected a spike time stamp and a waveform cutout spanning 1ms before and 2.2ms after the spike absolute maxima. The obtained waveform cutouts were sorted using the unsupervised Wave clus algorithm. After automatic clustering, we performed the suggested minor manual tuning to improve the sorting accuracy. All detected spikes for all conditions and timepoints were included in the spike sorting analysis. Statistics were calculated by one-way ANOVA followed by Tukey's multiple comparisons test.

Western Blot Analysis

We maintained sister cultures that were seeded and transduced in parallel to MEA cultures. Neurons were scrape-harvested on DIV21 into RIPA buffer (50 mM Tris-HCl pH 7.4, 150 mM NaCl, 1 mM EGTA, 1% NP-40, 0.25% sodium deoxycholate, 0.1% SDS, 1 mM phenylmethylsulfonyl fluoride). Cells were lysed by passing them through a 25½-gauge needle approximately 10 times. The lysates were placed on a nutator for 30 minutes at 4 °C, followed by a 15 minute spin at 13,000×*g* to pellet insoluble material. Proteins were resolved on a 10% SDS-polyacrylamide gel and transferred to a polyvinylidene difluoride membrane. The blot was probed with the indicated antibodies (Figure 1(C)).

Statistics

All data are presented as mean values ± standard error of the mean (s.e.m.), with *n* indicating the number of MEAs. All statistical analyses were performed using Prism 7.0 (GraphPad, La Jolla, CA) with $p<0.05$ representing statistical significance. D'Agostino-Pearson tests were performed to verify the normality assumption before ANOVA tests were used.

Results

Cypin increases proximal and distal dendrite branching independent of PSD-95 binding

We previously showed that cypin promotes dendrite branching and that the binding of cypin to PSD-95 regulates the placement and stability, but not the promotion, of dendrite branches [25]. To determine how cypin affects the overall arbor and whether it acts via binding to PSD-95, we overexpressed cypin or cypin lacking the PDZ-binding motif (cypinΔPDZ) in rat hippocampal neurons from DIV 7-12, a period of active proximal and distal branching [25, 26], and assessed the effect on dendrite branching. Total Sholl analysis suggests that overexpression of either cypin or cypinΔPDZ promotes proximal and distal dendrite branching during this developmental timepoint (Figure 2(A)). Cypin overexpression results in a significant increase in dendritic branches at 0-54 μm away from the soma, and cypinΔPDZ significantly increases branching in a similar manner (at 0-48 μm away from the soma; Figure 2(B)). As a result, the total number of dendrites significantly increases by DIV12 when either protein is expressed (Figure 2(C)). Interestingly, we observed that this increase observed in Total Sholl analysis is specific to the order of dendrite. While overexpression of cypin does not affect the number of primary or secondary dendrites (Figure 2(D, E)), it significantly increases the number of tertiary and higher order dendrites (Figure 2(F)). In contrast, neurons that overexpress cypinΔPDZ show a trend towards an increase in primary and tertiary and higher order dendrites. These data are consistent with our previous report that overexpression of cypin between DIV 6-10 results in an increase in both primary and tertiary and higher order dendrites [27]. Our data suggest that increases in dendrite numbers promoted by cypin at this timepoint are independent of PSD-95 binding.

Cypin overexpression decreases the number of dendritic spines

Dendritic spines are small protrusions in the membrane of dendrites that receive most of the excitatory synapses in the brain, and thus, understanding how cypin affects both dendrites and spines will aid in understanding of how it shapes neuronal circuits. Furthermore, since the presence and absence of PSD-95 puncta at the synapse correlate with spine formation, synapse formation, and pruning, and since we previously reported that cypin overexpression results in a decrease in PSD-95 puncta [5], we investigated the effect of altering cypin levels on the density and maturity of dendritic spines. We found that when cypin is overexpressed from DIV14-17, a time period when spine formation and maturation occurs in our cultures [28], the number of dendritic spines is reduced (Figure 3). Moreover, when cypinΔPDZ is overexpressed, there is a trend towards a decrease in dendritic spines compared to control ($p = 0.06$), but this is not statistically different from the spine density found after overexpression of cypin (Figure 3), suggesting that the interaction between cypin and PSD-95 is not essential for cypin-promoted changes to spines. Thus, our results suggest that

the PDZ-binding motif is only partially necessary for the observed reduction in dendritic spines after cypin overexpression.

Binding of cypin to PSD-95 influences spontaneous activity

To determine the effects of cypin overexpression on spontaneous activity, we performed whole-cell patch-clamp recordings of spontaneous excitatory postsynaptic currents (sEPSCs) in hippocampal neurons. We transduced neurons with lentivirus to either overexpress cypin or cypinΔPDZ on DIV14 and recorded sEPSCs at DIV21. Overexpression of cypin has no effect on sEPSCs (Figure 4(A,B)); however, overexpression of cypinΔPDZ results in a decrease in the frequency of sEPSCs (Figure 4(A,B)). Amplitude remains unchanged, regardless of which protein is overexpressed (Figure 4(A,C)). Interestingly, this suggests that the binding of cypin to PSD-95 or PSD-95 family members inhibits cypinΔPDZ-promoted inhibition of spontaneous activity. These results are surprising, and they indicate that although cypin alters postsynaptic spine density independent of PSD-95 binding, the binding of PSD-95 to cypin may modulate the effects of cypin at presynaptic sites.

Overexpression of cypin decreases bursting

Since overexpression of cypin has no effect on spontaneous activity, and since the binding of PSD-95 to cypin may inhibit an effect on sEPSC frequency, we asked whether cypin and its interaction with PSD-95 act to regulate bursting as a measure of how cypin affects neural circuit behavior. In contrast to having no influence on single cell sEPSCs, overexpression of cypin results in decreased burst frequency and increased burst width (Figure 5). Deletion of the PDZ-binding domain causes a significantly larger decrease in burst frequency with a similar increase in burst width (Figure 5). These data suggest that overexpression of cypin decreases bursting of single neurons in networks and that this bursting is further decreased when cypin is not in a complex with PSD-95, pointing to both PSD-95-dependent and independent roles for cypin in regulating circuitry.

Effect of Cypin Overexpression on the Spiking Activity of Cultured Hippocampal Neurons

To complement our work in single cells and to study network dynamics, we maintained high density hippocampal cultures on MEAs. Networks remained electrically active for at least three weeks, and we used lentiviral gene transfer to overexpress GFP-tagged cypin or cypin lacking the PDZ binding motif (cypinΔPDZ) at DIV10, when cypin increases dendrite branching (Figure 2 and [12, 29]), and allowed expression to continue to DIV17, when cypin influences spine density (Figure 3). Cultures overexpressing GFP were used as controls. Exogenous protein expression levels obtained with this approach were higher and more consistent than those obtained when attempting to use transfection due to the high density and age of the cultures. To confirm that recorded activity was transmitted synaptically, we recorded the electrical activity of the networks in the presence of a combination of synaptic blockers: 5 μM 6-cyano-7-nitroquinoxaline-2,3-dione (CNQX), 20 μM bicuculline, and 20 μM (2R)-amino-5-phosphonovaleric acid (APV) (Figure 6). The cocktail of synaptic blockers was added to the recording medium for the duration of the 5 minute equilibration period prior to recording. This treatment resulted in a dramatic decrease in the overall

spiking activity of the networks, confirming that the recorded activity resulted from action potentials induced by synaptic transmission.

The activity pattern of a neuronal network typically involves isolated spikes accompanied by bursting events, periods of high electrical activity when multiple electrodes display numerous action potentials during a short period of time [30]. We measured the overall spiking rate of the networks immediately before transduction on DIV10 (baseline), 7 days later (DIV17), and 11 days later (DIV21). We found that the overall spiking activity of cultures significantly decreases by DIV17 for control networks and networks overexpressing cypin, and remains at this lower level until DIV21 for control networks (Figure 7(A)). This global decrease in activity is consistent with the notion that during the establishment and maturation of synapses within neural circuits, connections undergo continuous modification and refinement [31, 32]. Early synaptic connections tend to be brief and frequent and give way to the more stable connections, characteristic of mature circuits. We calculated the average number of active spiking electrodes and found that it was similar for all timepoints and all conditions (Figure 7(B)), suggesting that the observed decrease in activity is due to a combination of developmental changes in the network and our experimental manipulations. We quantified the bursting and synchronous behavior of our networks and found no significant difference between groups or timepoints.

Although the number of active electrodes proved to be a stable measurement, we observed high trial-to-trial (recording session) variability associated with spiking data. This has been previously reported by others [21, 33] and was visually evident when monitoring the activity during recordings and when displaying the spike rate distribution of individual cultures. To determine if the initial level of spiking activity dictates how active a culture remains over time, we classified the cultures depending on the initial average number of spikes detected at DIV10 before transduction: low baseline (<2,000 spikes), intermediate baseline (2-10,000 spikes), and high baseline (>10,000 spikes) (Figures 8(B)-(E)). Since 2,000 spikes is a low activity threshold, we also analyzed intermediate and high baselines (>2,000 spikes) in combination to further elucidate if low baselines influence the observed global variability (Figure 8(C)).

We found that cultures with baselines under 2,000 spikes (Figure 8(B)) do not exhibit a significant change in the average spike rates over time for all conditions. When considering the group of cultures with baselines of >2,000 spikes (Figure 8(C)), it becomes evident that these networks behave almost identically to the overall group including all cultures (Figure 8(A)). These data imply that cultures with low baseline spiking do not make a large contribution to the overall spike rate reduction observed when considering the full distribution of spike rates. Similarly, the spike rate of networks with intermediate baselines (Figure 8(D)) remain relatively unchanged over time. Finally, cultures with initial high spike rates (Figure 8(E)) show significant reductions in activity by DIV17 and DIV21, regardless of the condition.

In summary, the spike rate of cultures with initially low or intermediate baselines are not affected by network development or cypin overexpression. In contrast, cultures with high baselines show reductions in spike rates over time for all conditions. Interestingly, the

average spike rate of networks that overexpress cypinΔPDZ only changes significantly at higher baselines. Our data suggest that the initial spike rate of neuronal networks influences the effect that overexpression has on activity over time.

Effect of Cypin Overexpression on the Spiking Variability of Cultured Hippocampal Neurons

We extended our analysis to the evaluation of spiking variability. This analysis has proven valuable in studies that range from *in vitro* networks [34] to animal experiments [22, 35, 36] to computational models [21, 37, 38]. We calculated the Fano factor as a measure of variability in the spike count and found that our networks exhibit average Fano factors of 3.03 - 3.10 at baseline, suggesting that the firing rate of the networks is inherently irregular at this timepoint (Figure 9(A)). Cypin overexpression significantly increases the Fano factor by DIV21, suggesting that although the mean spike rate of networks that overexpress cypin decreases over time, the mean variability in firing rate increases. High Fano factors have been observed in other systems [22], and it is not uncommon for an MEA study to report this level of spike count variability [39]. Highly clustered networks exhibit high Fano factors, raising the possibility that overexpression of cypin causes subsets of connected neurons in a network to become better connected functionally [21], introducing slow fluctuations in firing rate accompanied by high spiking variability.

We sought to determine whether variability in spike count is dependent on the initial spike rate. The relationship between spike rate and spike count variability for each network is summarized in Figures 9(B)-(D). For each culture, the Fano factor is plotted versus the spike rate. Hence, each line represents data from a single culture over time with one data point each for baseline (DIV10), DIV17, and DIV21. As seen in Figures 9(B)-(D), this relationship is highly variable within each condition over time and between conditions. In fact, we found that the distribution of Fano factors is significantly different in the control condition between baseline and DIV21 (Mann-Whitney U test, $p < 0.05$) and for cypin overexpression between baseline and DIV17 (Mann-Whitney U test, $p < 0.01$). The remaining Fano factor distributions do not show significant differences over time. We calculated the average non-parametric Spearman's rank correlation coefficients (Spearman's rho) for each condition and found no significant correlations between Fano factor and spike rate. The high trial-to-trial (recording session) variability found between different recording sessions renders this relationship difficult to interpret, yet differences in spike rate have been shown to influence spike count variability [40]. In light of our data, it is also important to note that high Fano factors have been observed in other systems [22], and it is not uncommon for an MEA study to report this level of spike count variability [39].

We then studied the relationship between these two parameters at different levels of initial spiking rate to determine if the baseline activity level influences the Fano factor over time (Figure 10). Because of the wide spread of data points along both axes, the mean ± s.e.m. is displayed. We classified the cultures depending on the initial average number of spikes detected as in Figure 8 and studied how the average Fano factor is influenced by level of firing over time. For each condition, the average Fano factor is plotted versus the average spike rate across the three timepoints; therefore, each line represents the average of data

from all of the cultures in a particular condition over time. Note that each line has 3 data points: a circle (baseline), a square (DIV17), and a triangle (DIV21).

To quantify the dependence of spike count variability on the mean spike rate, we calculated the Spearman's correlation coefficients for each condition at each timepoint and compared them using Fisher's Z-transformation [41]. We found that the coefficient of correlation of networks that overexpress cypin changes significantly ($p < 0.01$, $n = 6$) from baseline (Spearman's rho = -0.4286) to DIV21 (Spearman's rho = 0.6571) for intermediate baseline spike rates (Figure 10(D)). This suggests that for intermediate baseline spike rates, there is a negative relationship between variability and rate that significantly evolves into a positive relationship by DIV21 when cypin is overexpressed. Moreover, we found that the coefficient of correlation of networks that overexpress cypin changes significantly ($p < 0.01$, $n = 5$) from baseline (Spearman's rho = 0.5) to DIV17 (Spearman's rho = 1.0) for high baseline spike rates (Figure 10(E)). This is accompanied by a strong trend ($p = 0.0561$, $n = 5$) towards a decrease between DIV17 and DIV21 (Spearman's rho = 0.8). These data suggest that at high baseline spike rates, there is a positive relationship between Fano factor and spike rate that gets stronger by DIV17 before it becomes negative by DIV21. We found no significant changes in coefficients of correlation for networks overexpressing GFP or cypinΔPDZ for any initial spike rate level, suggesting that cypin mediates its effects, at least in part, by binding to PSD-95 or PSD-95 family members.

Changes in Spike Waveforms after Cypin Overexpression

Finally, we sought to uncover differences in our networks at the individual spike level. When analyzing data from multisite recordings, spike sorting allows us to decipher information from individual neurons that make up the signals detected by each recording site [42]. We used the spike sorting algorithm Wave_clus [23] to determine whether cypin overexpression results in differences in the shapes of spontaneous potentials detected by our networks over time. Spike sorting analysis resulted in five different spike waveforms: one negative and one positive monophasic waveform, two biphasic waveforms, and one triphasic waveform (Figure 11(A)).

Neuronal networks coupled to planar electrodes on MEAs are known to fire mostly negative spikes, accompanied by a lower proportion of positive spikes [43]. Our results are consistent with this throughout the 21 days in culture (Figure 11(B)-(D)). We found that by DIV17 (Figure 11C), networks in all conditions gained one new type of spike waveform when compared to baseline. By DIV21, networks that overexpress cypin exhibit a new type of spike waveform, the negative triphasic spike, which is not present in any of the other conditions (Figure 11D). In fact, networks that overexpress GFP or cypinΔPDZ show a distribution of spikes that resembles their respective baselines, and networks that overexpress GFP show a decrease in spike waveform distribution complexity. Thus, the changes in spike waveforms observed after cypin overexpression may be dependent on PSD-95 family member binding.

Discussion

Cypin is a multifunctional protein that functions to decrease PSD-95 localization at the synapse [5]. In addition, it acts to metabolize guanine and promote dendrite branching by binding tubulin heterodimers and promoting microtubule assembly [29, 44]. Since PSD-95 plays an integral role in synapse assembly and maturation [4, 45], we used multiple assays in this study to determine the role of cypin in shaping single neurons and the neuronal network. We found that the binding of cypin to PSD-95 is dispensable for promoting dendrite branching and reducing spine density; however, the interaction between the two proteins plays a role in spontaneous single cell activity and network activity. First, although overexpression of cypin has no effect on the spontaneous activity of single neurons, blocking interaction of cypin with PSD-95 by deleting the PDZ-binding domain on cypin decreases sEPSC frequency (Figure 4), suggesting an inhibitory role for the interaction of cypin with PSD-95. Similarly, overexpression of cypin decreases single neuron bursting, and inhibiting PSD-95 binding decreases bursting further (Figure 5). Interestingly, when we used MEAs to examine the functional consequence of overexpressing cypin or the mutant cypinΔPDZ in hippocampal neuronal networks, we found that disrupting the interaction between cypin and PSD-95 attenuated all cypin-promoted changes to the network.

Our spike sorting analysis revealed that cypin overexpression leads to the presence of spike waveforms that are absent in control networks and networks overexpressing cypinΔPDZ. Networks in all conditions exhibit an expected majority of negative waveforms, accompanied by some positive waveforms. Negative peaks reflect inward currents recorded mainly from axons and excitable soma, and positive field potentials are associated with outward currents from dendrites [43, 46]. However, cypin overexpression also results in the presence of negative triphasic spikes by DIV21. The polarity and shape of spike waveforms are dependent on many factors, such as morphology of the dendritic tree, the distance between the spiking neuron and the recording electrode, the coupling between neurons and electrodes, and the properties of the recording medium [47]. Neuron-electrode coupling, distance, and recording medium composition are factors that would affect all cultures equally. Hence, we assume that the observed changes in spike waveforms in our networks are not random and result from a combination of exogenous protein expression and regular network development. Negative spikes that are characterized by positive components have been associated with electrodes that are in close vicinity to dendritic segments [48]. Hence, it is plausible that the enhanced dendritic arbor present in cypin-overexpressing networks is responsible for some or all of the spike waveform changes observed.

Based on these data, a possibility is that cypin overexpression leads to changes in network properties simply by promoting dendritogenesis. Interestingly, our results do not support this idea. Overexpression of cypin promotes dendrite branching as does overexpression of cypinΔPDZ, although the placement and stability of these branches appear to differ [25]. At the single cell level, cypin binding to PSD-95 serves to inhibit cypin-promoted changes to sEPSCs and bursting. Similarly, at the network level, as determined by MEA recordings, disrupting PSD-95 binding to cypin attenuates the effects of cypin on the network for all parameters examined. Since overexpression of either cypin or cypinΔPDZ increases dendrites, this change cannot account for all of the cypin-promoted changes to the network.

It would be ideal to determine the relationship between the morphology changes in the individual cells and to those in the network. Viral transduction is necessary to obtain cypin expression in the majority of cells in the network, which are cultured at high density on MEAs and do not allow for single neuron tracing. In contrast, our morphological analysis depends on <10% transfection efficiency by lipid-mediated transfection, and thus, it was not possible to perform this same analysis for our MEA cultures. Future experiments will extend our use of single cell electrophysiology to determine how changes to the dendritic arbor correlate with changes to miniature and spontaneous excitatory postsynaptic currents.

How can cypin act to alter neuronal function or network activity? Cypin binds zinc [29, 44], which is found in dendritic shafts and spine heads and stabilizes microtubules [49]. Cypin also binds to tubulin heterodimers and promotes microtubule assembly [29]. Dendrites are microtubule-rich, and it was recently reported that microtubules are highly dynamic and polymerize in dendritic spines [50-52]. Lack of KIF21B, a microtubule motor, results in deficits in synaptic transmission [53]. In dendrites and spines, microtubules are involved in trafficking of lysosomes in an activity-dependent manner, where the lysosomes regulate turnover of synaptic membrane proteins, specifically glutamate receptors [54]. Thus, changes to microtubule polymerization and dynamics by cypin may play a role in changes to single cell and network activity by altering microtubule-dependent processes in spines.

Cypin also binds to the SNARE-associated protein snapin, a protein present at both pre-and postsynaptic sites [55]. Snapin was originally identified as a SNAP-25-binding protein and as a modulator of neurotransmitter release [56]. It is also part of the biogenesis of lysosome-related organelles complex-1 (BLOC-1) [57]. Snapin is phosphorylated by cAMP-dependent protein kinase (PKA), and this phosphorylation regulates its interaction with SNAP-25 [58, 59] and cypin [55]. Recently, snapin has been found to play a role in autophagy [60, 61] and to regulate synaptic activity by regulating endolysosomal transport and sorting [62]. Thus, cypin may play a PSD-95-indpendent role in regulating synaptic and network activity via interaction with snapin.

PSD-95 binding to cypin inhibits cypin-promoted effects to spontaneous activity in single neurons, but on the other hand, is responsible for effects on the network. This is not surprising given the fact that PSD-95 exhibits synapse specificity and that the functional defects resulting from the deletion of the PDZ-binding motif in cypin may be restricted to only a subset of synapses [8]. However, why would cypin act differently to regulate activity of single neurons versus networks? We believe that it is possible that the synaptic defect that results from knocking down synaptic PSD-95 via cypin overexpression may affect a small population of synapses and that other members of the MAGUK family of proteins may compensate for decreases in synaptic PSD-95 localization.

Lack of the PDZ-binding site in cypin, and therefore, lack of PSD-95 binding, would increase PSD-95 clustering at the postsynaptic site. This increase, in effect, could lead to increased numbers of AMPA and NMDA receptors at postsynaptic sites, leading to scaling and overall decrease in sEPSC frequency. Furthermore, disruption of the binding of snapin to SNAP-25 reduces frequency of neurotransmission and amplitude of sEPSCs [63]. These data, therefore, suggest that the binding of cypin to snapin does not necessarily decrease

snapin function, and the presynaptic effect observed with expression of cypinΔPDZ is due to homeostasis [64]. Specifically, expression of cypinΔPDZ results in decreased frequency compared to overexpression of cypin but not to control. If this were not the case, the data would suggest that cypinΔPDZ can bind snapin and prevent stabilization of synaptic vesicles [65], reducing neurotransmission. Reduction in bursting frequency and duration suggests even further a homeostatic effect that tunes the network activity down but increases its synchrony. Cypin increases dendritic branching, therefore, increase in synaptic connections between large number of neurons may increase network synchrony [66].

We observed that the overall rate of isolated spikes decreases by DIV17 for control networks and for networks overexpressing cypin and stabilizes until DIV21 for control networks. As networks mature, their firing rate is known to plateau [31, 32], which could explain the lack of change in activity from DIV17 to DIV21. Moreover, given the high cell density of our cultures and period of time between transduction and recordings, it is possible that compensatory mechanisms were present and the networks reached homeostasis during the first seven days after transduction [67]. A more detailed examination of the change in spike rate revealed that exogenous protein expression has slightly different effects on network activity, depending on the initial spike rate. Cultures with low or intermediate baseline spike rates are not affected by cypin overexpression, whereas cultures with high baseline spike rates exhibit significant decreases in spiking activity over time for all conditions. These results suggest that only analyzing the average influence of cypin overexpression for all networks may not be an effective method for understanding its action on networks and that taking into account the trial-to-trial variability between recording sessions reveals patterns that are otherwise masked by averaging.

Moreover, it is possible that cypin overexpression accelerates maturation of the network. We have previously shown that cypin overexpression significantly increases dendrite branching (i.e. [12, 25, 29]), and a consequence of this morphological change may be to accelerate the maturation of the network without changing the final state. Our current study confirms these morphological findings, adding to them that the PDZ-binding motif is not necessary for increasing dendrite branching during the active branching period (DIV7-12) [12, 25, 29, 68, 69]. Additionally, our current study shows that during the next stage of development (DIV14-17), cypin overexpression decreases spine density, but only when the PDZ domain is present. Several studies have shown that pruning of spines, and therefore synapses, occurs during development [70-74]. Thus, it is possible that cypin promotes maturation of hippocampal networks at both earlier and later stages of development, albeit through different mechanisms. Since viral overexpression of cypin begins at DIV10 for neurons cultured on MEAs, it is possible that cypin causes a combination of morphological changes, by altering both dendrites and spines, and that this, in part, explains the activity-dependent changes observed during MEA recordings.

We used the Fano factor as a measure of spiking variability and found that networks that overexpress cypin exhibit higher spike count variability by DIV21. In contrast, the spike count variability of networks overexpressing GFP or cypinΔPDZ does not change significantly over time. Importantly, our dendrite branching data suggest that increased spiking variability is not simply a phenomenon generated by the increased branching of the

dendrites. If this were the case, we would expect networks overexpressing cypinAPDZ to have also shown increased spike rate variability. We suspect that the reason networks overexpressing cypin and cypinAPDZ differ in how their Fano factors change has more to do with changes in single neuron activity than in dendrite morphology. We observed decreases in spine density after cypin overexpression, but not after cypinAPDZ overexpression, which may be one of the reasons Fano factor increased in these networks. Future work will attempt to directly correlate changes in individual neuron spike rates, using either single cell electrophysiology or calcium imaging, with changes in overall network activity.

Our networks display high Fano factors even at baseline, which is potentially a result of the high cell density of our cultures and the intrinsic variability of spontaneous neuronal activity [75]. The Fano factor decreases as the mean firing rate increases in multiunit recordings, reflecting an underlying variance in the firing rate [22]. In addition, computational models correlate an increase in spike count variability with higher clustering between neurons in a network [21]. Our results suggest that networks overexpressing cypin could exhibit higher neuronal clustering and undergo more dramatic firing fluctuations, as some clusters within the network transition to and from low to high activity levels, causing the overall spike count variability to increase. This could also explain the changes in dependence of Fano factor on spike rate that we observed only for networks that overexpress cypin. Finally, the effect of cypin overexpression on Fano factor may be related to network maturation and the ability of networks to carry information. Neuronal networks undergo changes in firing rate and synchronization during maturation [76-78] that affect functionality [79]. Since the networks used in this study are derived from embryonic rat neurons, they are still very young and undergoing maturation. Thus, while the Fano factors presented in this study are considered high (>1), it is possible that this metric may decrease over time as the network matures. Studies of the auditory cortex in awake, behaving rats, for example, indicate that an increase in Fano factor leads to a decrease in information processing [80]. Future work will attempt to quantify information processing in our *in vitro* networks using MEAs and other electrophysiology techniques to understand the effect of altering gene expression on circuit functionality.

Conclusion

Our group previously identified and characterized cypin as regulator of the synaptic localization of a key component of postsynaptic sites, PSD-95. Cypin is also a core regulator of dendrite branching. In this study, we explored the functional implications of altering cypin levels on neuronal network dynamics. We show successful use of lentiviral gene transfer to achieve network-wide exogenous protein expression in high density hippocampal cultures. Our results suggest that increases in dendrite branching do not necessarily correlate with changes to network activity. We found that cypin, a protein that increases dendrites, results in no change in spontaneous activity at the single cell level but that it decreases single cell bursting and increases network spike rate and variability. Highly clustered networks exhibit high Fano factors, raising the possibility that overexpression of cypin causes subsets of connected neurons in a network to become better connected functionally [29]. Importantly, binding of PSD-95 to cypin, via expression of cypinΔPDZ, inhibits changes to sEPSCs and further decreases bursting activity. In contrast, PSD-95 binding is necessary for

cypin-promoted effects on network spike rate and variability. Since overexpression of cypin and cypinΔPDZ show similar effects on dendrite branching and spine density, taken together, our results suggest that dendrite morphology does not play a major role in the action of cypin on electrical activity, perhaps pointing to a role for cypin-promoted microtubule assembly, zinc binding, or interaction with snapin. These potential mechanisms are currently being explored.

Acknowledgments

This work is funded in part by National Science Foundation grant IOS-1353724 and New Jersey Commission on Brain Injury Research grant #CBIR14IRG019 (to BLF). AR, KMO, and PS are supported by the National Institutes of Health under the Ruth L. Kirschstein National Research Service Award T32 GM8339 from the NIGMS. KMO is also supported by a Predoctoral Fellowship from the New Jersey Commission on Brain Injury Research #CBIR13FEL002 and a Predoctoral GAANN Fellowship #P200A150131 from the DOE. PS is supported by a Predoctoral Fellowship from the New Jersey Commission on Brain Injury Research #CBIR16FEL013, and MP is supported by a Predoctoral Fellowship from the New Jersey Commission on Brain Injury Research #CBIR15FEL009.

References

1. Vetter P, Roth A, Hausser M. Propagation of action potentials in dendrites depends on dendritic morphology. Journal of neurophysiology. 2001; 85(2):926–37. [PubMed: 11160523]
2. Sheng, M. Molecular organization of the postsynaptic specialization; Proceedings of the National Academy of Sciences of the United States of America; 2001; p. 7058-61.
3. Kulkarni VA, Firestein BL. The dendritic tree and brain disorders. Molecular and cellular neurosciences. 2012; 50(1):10–20. [PubMed: 22465229]
4. El-Husseini AE, Schnell E, Chetkovich DM, Nicoll RA, Bredt DS. PSD-95 involvement in maturation of excitatory synapses. Science (New York, N Y). 2000; 290(5495):1364–8.
5. Firestein BL, Brenman JE, Aoki C, Sanchez-Perez AM, El-Husseini AED, Bredt D. Cypin: a cytosolic regulator of PSD-95 postsynaptic targeting. Neuron. 1999; 24:659–672. [PubMed: 10595517]
6. Migaud M, Charlesworth P, Dempster M, Webster LC, Watabe AM, Makhinson M, He Y, Ramsay MF, Morris RG, Morrison JH, O'Dell TJ, Grant SG. Enhanced long-term potentiation and impaired learning in mice with mutant postsynaptic density-95 protein. Nature. 1998; 396(6710):433–9. [PubMed: 9853749]
7. Bredt DS, Nicoll RA. AMPA receptor trafficking at excitatory synapses. Neuron. 2003; 40(2):361–79. [PubMed: 14556714]
8. Beique, JC., Lin, DT., Kang, MG., Aizawa, H., Takamiya, K., Huganir, RL. Synapse-specific regulation of AMPA receptor function by PSD-95; Proceedings of the National Academy of Sciences of the United States of America; 2006; p. 19535-40.
9. Keith D, El-Husseini A. Excitation Control: Balancing PSD-95 Function at the Synapse. Frontiers in molecular neuroscience. 2008; 1:4. [PubMed: 18946537]
10. Yudowski GA, Olsen O, Adesnik H, Marek KW, Bredt DS. Acute inactivation of PSD-95 destabilizes AMPA receptors at hippocampal synapses. PloS one. 2013; 8(1):e53965. [PubMed: 23342049]
11. Schnell, E., Sizemore, M., Karimzadegan, S., Chen, L., Bredt, DS., Nicoll, RA. Direct interactions between PSD-95 and stargazin control synaptic AMPA receptor number; Proceedings of the National Academy of Sciences of the United States of America; 2002; p. 13902-7.
12. O'Neill KM, Akum BF, Dhawan ST, Kwon M, Langhammer CG, Firestein BL. Assessing effects on dendritic arborization using novel Sholl analyses. Front Cell Neurosci. 2015; 9:285. [PubMed: 26283921]
13. Sweet ES, Langhammer CL, Kutzing MK, Firestein BL. Semiautomated analysis of dendrite morphology in cell culture. Methods Mol Biol. 2013; 1018:261–8. [PubMed: 23681635]

14. Kutzing MK, Langhammer CG, Luo V, Lakdawala H, Firestein BL. Automated Sholl analysis of digitized neuronal morphology at multiple scales. J Vis Exp. 2010; (45)
15. Langhammer CG, Previtera ML, Sweet ES, Sran SS, Chen M, Firestein BL. Automated Sholl analysis of digitized neuronal morphology at multiple scales: Whole cell Sholl analysis versus Sholl analysis of arbor subregions. Cytometry A. 2010; 77(12):1160–8. [PubMed: 20687200]
16. Hernandez K, Swiatkowski P, Patel MV, Liang C, Dudzinski NR, Brzustowicz LM, Firestein BL. Overexpression of Isoforms of Nitric Oxide Synthase 1 Adaptor Protein, Encoded by a Risk Gene for Schizophrenia, Alters Actin Dynamics and Synaptic Function. Frontiers in cellular neuroscience. 2016; 10:6. [PubMed: 26869880]
17. Kutzing MK, Luo V, Firestein BL. Measurement of synchronous activity by microelectrode arrays uncovers differential effects of sublethal and lethal glutamate concentrations on cortical neurons. Ann Biomed Eng. 2011; 39(8):2252–62. [PubMed: 21544673]
18. Kutzing MK, Luo V, Firestein BL. Protection from glutamate-induced excitotoxicity by memantine. Ann Biomed Eng. 2012; 40(5):1170–81. [PubMed: 22203191]
19. Eden UT, Kramer MA. Drawing inferences from Fano factor calculations. Journal of neuroscience methods. 2010; 190(1):149–52. [PubMed: 20416340]
20. Gambazzi L, Gokce O, Seredenina T, Katsyuba E, Runne H, Markram H, Giugliano M, Luthi-Carter R. Diminished activity-dependent brain-derived neurotrophic factor expression underlies cortical neuron microcircuit hypoconnectivity resulting from exposure to mutant huntingtin fragments. The Journal of pharmacology and experimental therapeutics. 2010; 335(1):13–22. [PubMed: 20624994]
21. Litwin-Kumar A, Doiron B. Slow dynamics and high variability in balanced cortical networks with clustered connections. Nature neuroscience. 2012; 15(11):1498–505. [PubMed: 23001062]
22. Churchland MM, Yu BM, Cunningham JP, Sugrue LP, Cohen MR, Corrado GS, Newsome WT, Clark AM, Hosseini P, Scott BB, Bradley DC, Smith MA, Kohn A, Movshon JA, Armstrong KM, Moore T, Chang SW, Snyder LH, Lisberger SG, Priebe NJ, Finn IM, Ferster D, Ryu SI, Santhanam G, Sahani M, Shenoy KV. Stimulus onset quenches neural variability: a widespread cortical phenomenon. Nature neuroscience. 2010; 13(3):369–78. [PubMed: 20173745]
23. Quiroga RQ, Nadasdy Z, Ben-Shaul Y. Unsupervised spike detection and sorting with wavelets and superparamagnetic clustering. Neural computation. 2004; 16(8):1661–87. [PubMed: 15228749]
24. Rey HG, Pedreira C, Quian Quiroga R. Past, present and future of spike sorting techniques. Brain research bulletin. 2015; 119(Pt B):106–17. [PubMed: 25931392]
25. Charych EI, Akum BF, Goldberg JS, Jornsten RJ, Rongo C, Zheng JQ, Firestein BL. Activity-independent regulation of dendrite patterning by postsynaptic density protein PSD-95. The Journal of neuroscience: the official journal of the Society for Neuroscience. 2006; 26(40):10164–76. [PubMed: 17021172]
26. Dotti CG, Sullivan CA, Banker GA. The establishment of polarity by hippocampal neurons in culture. The Journal of neuroscience: the official journal of the Society for Neuroscience. 1988; 8(4):1454–68. [PubMed: 3282038]
27. O'Neill KM, Akum BF, Dhawan ST, Kwon M, Langhammer CG, Firestein BL. Assessing effects on dendritic arborization using novel Sholl analyses. Frontiers in cellular neuroscience. 2015; 9:285. [PubMed: 26283921]
28. Ziv NE, Smith SJ. Evidence for a role of dendritic filopodia in synaptogenesis and spine formation. Neuron. 1996; 17(1):91–102. [PubMed: 8755481]
29. Akum BF, Chen M, Gunderson SI, Riefler GM, Scerri-Hansen MM, Firestein BL. Cypin regulates dendrite patterning in hippocampal neurons by promoting microtubule assembly. Nat Neurosci. 2004; 7(2):145–52. [PubMed: 14730308]
30. Raichman N, Ben-Jacob E. Identifying repeating motifs in the activation of synchronized bursts in cultured neuronal networks. Journal of neuroscience methods. 2008; 170(1):96–110. [PubMed: 18281097]
31. Tau GZ, Peterson BS. Normal development of brain circuits. Neuropsychopharmacology: official publication of the American College of Neuropsychopharmacology. 2010; 35(1):147–68. [PubMed: 19794405]

32. Biffi E, Regalia G, Menegon A, Ferrigno G, Pedrocchi A. The influence of neuronal density and maturation on network activity of hippocampal cell cultures: a methodological study. PloS one. 2013; 8(12):e83899. [PubMed: 24386305]
33. Kapucu FE, Tanskanen JMA, Mikkonen JE, Yla-Outinen L, Narkilahti S, Hyttinen JAK. Burst analysis tool for developing neuronal networks exhibiting highly varying action potential dynamics. Frontiers in computational neuroscience. 2012; 6:38. [PubMed: 22723778]
34. Becchetti A, Gullo F, Bruno G, Dossi E, Lecchi M, Wanke E. Exact distinction of excitatory and inhibitory neurons in neural networks: a study with GFP-GAD67 neurons optically and electrophysiologically recognized on multielectrode arrays. Frontiers in neural circuits. 2012; 6:63. [PubMed: 22973197]
35. Lei H, Reisenman CE, Wilson CH, Gabbur P, Hildebrand JG. Spiking patterns and their functional implications in the antennal lobe of the tobacco hornworm Manduca sexta. PloS one. 2011; 6(8):e23382. [PubMed: 21897842]
36. White B, Abbott LF, Fiser J. Suppression of cortical neural variability is stimulus-and state-dependent. Journal of neurophysiology. 2012; 108(9):2383–92. [PubMed: 22896720]
37. Christodoulou C, Cleanthous A. Does high firing irregularity enhance learning? Neural computation. 2011; 23(3):656–63. [PubMed: 21162670]
38. Moreno-Bote R. Poisson-like spiking in circuits with probabilistic synapses. PLoS computational biology. 2014; 10(7):e1003522. [PubMed: 25032705]
39. Weir K, Blanquie O, Kilb W, Luhmann HJ, Sinning A. Comparison of spike parameters from optically identified GABAergic and glutamatergic neurons in sparse cortical cultures. Frontiers in cellular neuroscience. 2014; 8:460. [PubMed: 25642167]
40. Vogel A, Hennig RM, Ronacher B. Increase of neuronal response variability at higher processing levels as revealed by simultaneous recordings. J Neurophysiol. 2005; 93(6):3548–59. [PubMed: 15716366]
41. L M, MJ S. Differences between Spearman Correlation Coefficients. Encyclopedia of Statistical Sciences. 2006; 12:1–2.
42. Harris KD, Quiroga RQ, Freeman J, Smith SL. Improving data quality in neuronal population recordings. Nat Neurosci. 2016; 19(9):1165–74. [PubMed: 27571195]
43. Fendyur A, Mazurski N, Shappir J, Spira ME. Formation of Essential Ultrastructural Interface between Cultured Hippocampal Cells and Gold Mushroom-Shaped MEA- Toward “IN-CELL” Recordings from Vertebrate Neurons. Front Neuroeng. 2011; 4:14. [PubMed: 22163219]
44. Fernandez JR, Welsh WJ, Firestein BL. Structural characterization of the zinc binding domain in cytosolic PSD-95 interactor (cypin): Role of zinc binding in guanine deamination and dendrite branching. Proteins. 2008; 70(3):873–81. [PubMed: 17803218]
45. Won S, Levy JM, Nicoll RA, Roche KW. MAGUKs: multifaceted synaptic organizers. Curr Opin Neurobiol. 2017; 43:94–101. [PubMed: 28236779]
46. Nam Y, Wheeler BC. In vitro microelectrode array technology and neural recordings. Crit Rev Biomed Eng. 2011; 39(1):45–61. [PubMed: 21488814]
47. Gold C, Henze DA, Koch C, Buzsaki G. On the origin of the extracellular action potential waveform: A modeling study. J Neurophysiol. 2006; 95(5):3113–28. [PubMed: 16467426]
48. Csicsvari J, Hirase H, Czurko A, Mamiya A, Buzsaki G. Oscillatory coupling of hippocampal pyramidal cells and interneurons in the behaving Rat. J Neurosci. 1999; 19(1):274–87. [PubMed: 9870957]
49. Perrin L, Roudeau S, Carmona A, Domart F, Petersen JD, Bohic S, Yang Y, Cloetens P, Ortega R. Zinc and Copper Effects on Stability of Tubulin and Actin Networks in Dendrites and Spines of Hippocampal Neurons. ACS Chem Neurosci. 2017
50. Jaworski J, Kapitein LC, Gouveia SM, Dortland BR, Wulf PS, Grigoriev I, Camera P, Spangler SA, Di Stefano P, Demmers J, Krugers H, Defilippi P, Akhmanova A, Hoogenraad CC. Dynamic microtubules regulate dendritic spine morphology and synaptic plasticity. Neuron. 2009; 61(1):85–100. [PubMed: 19146815]
51. Gu J, Firestein BL, Zheng JQ. Microtubules in dendritic spine development. J Neurosci. 2008; 28(46):12120–4. [PubMed: 19005076]

52. Hu X, Viesselmann C, Nam S, Merriam E, Dent EW. Activity-dependent dynamic microtubule invasion of dendritic spines. J Neurosci. 2008; 28(49):13094–105. [PubMed: 19052200]
53. Muhia M, Thies E, Labonte D, Ghiretti AE, Gromova KV, Xompero F, Lappe-Siefke C, Hermans-Borgmeyer I, Kuhl D, Schweizer M, Ohana O, Schwarz JR, Holzbaur EL, Kneussel M. The Kinesin KIF21B Regulates Microtubule Dynamics and Is Essential for Neuronal Morphology, Synapse Function, and Learning and Memory. Cell Rep. 2016; 15(5):968–77. [PubMed: 27117409]
54. Goo MS, Sancho L, Slepak N, Boassa D, Deerinck TJ, Ellisman MH, Bloodgood BL, Patrick GN. Activity-dependent trafficking of lysosomes in dendrites and dendritic spines. J Cell Biol. 2017
55. Chen M, Lucas KG, Akum BF, Balasingam G, Stawicki TM, Provost JM, Riefler GM, Jornsten RJ, Firestein BL. A novel role for snapin in dendrite patterning: interaction with cypin. Mol Biol Cell. 2005; 16(11):5103–14. [PubMed: 16120643]
56. Ilardi JM, Mochida S, Sheng ZH. Snapin: a SNARE-associated protein implicated in synaptic transmission. Nat Neurosci. 1999; 2(2):119–24. [PubMed: 10195194]
57. Starcevic M, Dell'Angelica EC. Identification of snapin and three novel proteins (BLOS1, BLOS2, and BLOS3/reduced pigmentation) as subunits of biogenesis of lysosome-related organelles complex-1 (BLOC-1). J Biol Chem. 2004; 279(27):28393–401. [PubMed: 15102850]
58. Chheda MG, Ashery U, Thakur P, Rettig J, Sheng ZH. Phosphorylation of Snapin by PKA modulates its interaction with the SNARE complex. Nat Cell Biol. 2001; 3(4):331–8. [PubMed: 11283605]
59. Thakur P, Stevens DR, Sheng ZH, Rettig J. Effects of PKA-mediated phosphorylation of Snapin on synaptic transmission in cultured hippocampal neurons. J Neurosci. 2004; 24(29):6476–81. [PubMed: 15269257]
60. Shi B, Huang QQ, Birkett R, Doyle R, Dorfleutner A, Stehlik C, He C, Pope RM. SNAPIN is critical for lysosomal acidification and autophagosome maturation in macrophages. Autophagy. 2017; 13(2):285–301. [PubMed: 27929705]
61. Cheng XT, Zhou B, Lin MY, Cai Q, Sheng ZH. Axonal autophagosomes recruit dynein for retrograde transport through fusion with late endosomes. J Cell Biol. 2015; 209(3):377–86. [PubMed: 25940348]
62. Di Giovanni J, Sheng ZH. Regulation of synaptic activity by snapin-mediated endolysosomal transport and sorting. EMBO J. 2015; 34(15):2059–77. [PubMed: 26108535]
63. Ilardi JM, Mochida S, Sheng ZH. Snapin: a SNARE-associated protein implicated in synaptic transmission. Nature neuroscience. 1999; 2(2):119–24. [PubMed: 10195194]
64. Dickman DK, Tong A, Davis GW. Snapin is critical for presynaptic homeostatic plasticity. The Journal of neuroscience: the official journal of the Society for Neuroscience. 2012; 32(25):8716–24. [PubMed: 22723711]
65. Yu SC, Klosterman SM, Martin AA, Gracheva EO, Richmond JE. Differential roles for snapin and synaptotagmin in the synaptic vesicle cycle. PloS one. 2013; 8(2):e57842. [PubMed: 23469084]
66. Takahashi N, Sasaki T, Matsumoto W, Matsuki N, Ikegaya Y. Circuit topology for synchronizing neurons in spontaneously active networks. Proceedings of the National Academy of Sciences of the United States of America. 2010; 107(22):10244–9. [PubMed: 20479225]
67. Fong MF, Newman JP, Potter SM, Wenner P. Upward synaptic scaling is dependent on neurotransmission rather than spiking. Nat Commun. 2015; 6:6339. [PubMed: 25751516]
68. Cline HT. Dendritic arbor development and synaptogenesis. Current opinion in neurobiology. 2001; 11(1):118–26. [PubMed: 11179881]
69. Wong ROL, Ghosh A. Activity-dependent regulation of dendritic growth and patterning. Nature reviews Neuroscience. 2002; 3(10):803–12. [PubMed: 12360324]
70. Bourgeois JP, Rakic P. Changes of synaptic density in the primary visual cortex of the macaque monkey from fetal to adult stage. The Journal of neuroscience: the official journal of the Society for Neuroscience. 1993; 13(7):2801–20. [PubMed: 8331373]
71. Rakic P, Bourgeois JP, Goldman-Rakic PS. Synaptic development of the cerebral cortex: implications for learning, memory, and mental illness. Progress in brain research. 1994; 102:227–43. [PubMed: 7800815]

72. Innocenti GM. Exuberant development of connections, and its possible permissive role in cortical evolution. Trends in neurosciences. 1995; 18(9):397–402. [PubMed: 7482805]

73. Huttenlocher PR. Synaptic density in human frontal cortex - developmental changes and effects of aging. Brain research. 1979; 163(2):195–205. [PubMed: 427544]

74. Huttenlocher PR, de Courten C. The development of synapses in striate cortex of man. Human neurobiology. 1987; 6(1):1–9. [PubMed: 3583840]

75. Hartmann C, Lazar A, Nessler B, Triesch J. Where's the Noise? Key Features of Spontaneous Activity and Neural Variability Arise through Learning in a Deterministic Network. PLoS Comput Biol. 2015; 11(12):e1004640. [PubMed: 26714277]

76. Maeda E, Robinson HP, Kawana A. The mechanisms of generation and propagation of synchronized bursting in developing networks of cortical neurons. The Journal of neuroscience: the official journal of the Society for Neuroscience. 1995; 15(10):6834–45. [PubMed: 7472441]

77. Pfeffer CK, Stein V, Keating Dj, Maier H, Rinke I, Rudhard Y, Hentschke M, Rune GM, Jentsch TJ, Hubner CA. NKCC1-dependent GABAergic excitation drives synaptic network maturation during early hippocampal development. The Journal of neuroscience: the official journal of the Society for Neuroscience. 2009; 29(11):3419–30. [PubMed: 19295148]

78. Uhlhaas PJ, Roux F, Rodriguez E, Rotarska-Jagiela A, Singer W. Neural synchrony and the development of cortical networks. Trends in cognitive sciences. 2010; 14(2):72–80. [PubMed: 20080054]

79. Uhlhaas PJ, Roux F, Singer W, Haenschel C, Sireteanu R, Rodriguez E. The development of neural synchrony reflects late maturation and restructuring of functional networks in humans. Proceedings of the National Academy of Sciences of the United States of America. 2009; 106(24): 9866–71. [PubMed: 19478071]

80. Abolafia JM, Martinez-Garcia M, Deco G, Sanchez-Vives MV. Variability and information content in auditory cortex spike trains during an interval-discrimination task. Journal of neurophysiology. 2013; 110(9):2163–74. [PubMed: 23945780]

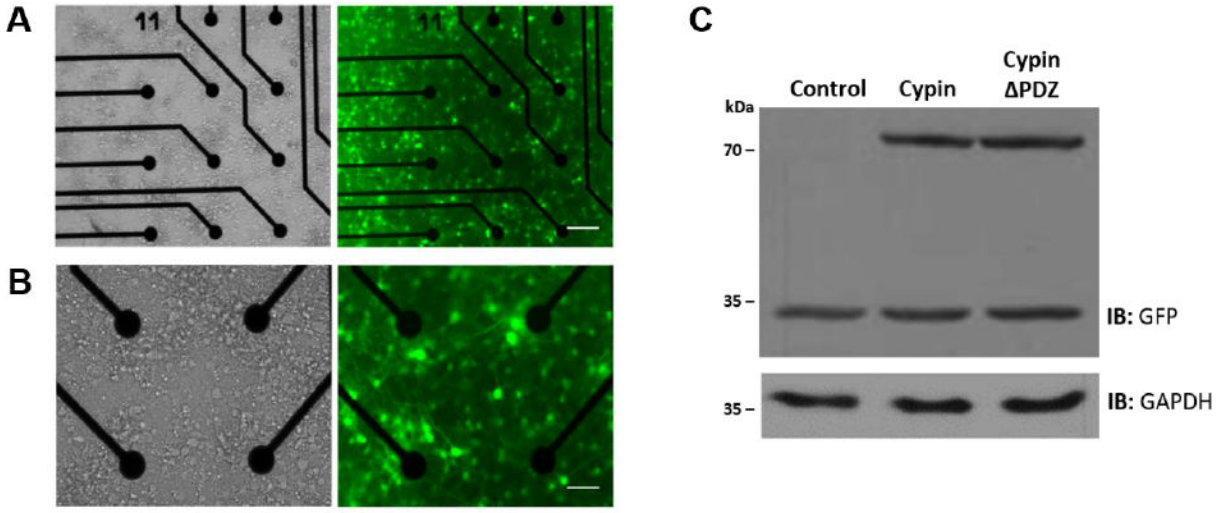

Figure 1. Transduced cultures on MEAs at DIV17 exhibit a high proportion of GFP-positive neurons

All transduced MEAs were visually inspected under a fluorescence microscope to confirm successful transduction based on GFP expression. (A) Representative brightfield and fluorescence images (100X) of transduced MEA cultures at DIV17. Scale bar is 100 μm. (B) Higher magnification (200X) confirms that a high fraction of the cultured neurons express GFP. Scale bar is 50 μm. (C) Sister cultures were maintained in parallel to MEA cultures and Western blotting was performed at DIV21. Representative blots show successful transduction as determined by probing with an antibody against GFP. GAPDH (~37 kDa) was used as a loading control. The predicted size of GFP-tagged cypin protein is ~78 kDa and the predicted size of GFP is ~28 kDa.

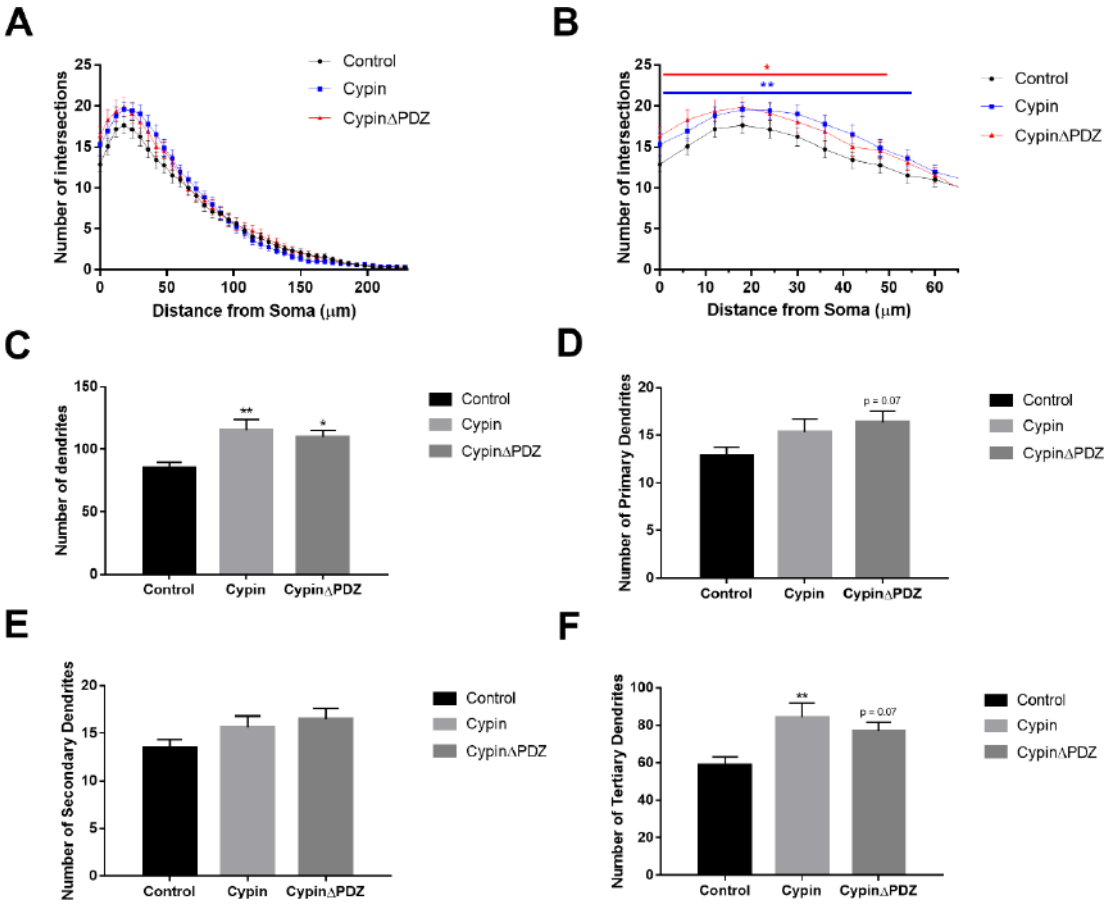

Figure 2. Proximal and distal dendrite branching are increased by overexpression of cypin, independent of PSD-95 binding

(A) Total Sholl analysis shows increased dendrite branching when cypin or cypinΔPDZ is overexpressed from DIV7-12. (B) Sholl analysis of dendrites within 60 μm of the soma shows that cypin overexpression increases branching at 0-54 μm away from the soma (**$p < 0.01$) and that cypinΔPDZ increases branching at 0-48 μm away from the soma (*$p < 0.05$). (C) Overexpression of cypin or cypinΔPDZ increases the total number of dendrites. Overexpression of cypin or cypinΔPDZ does not result in significantly increase (D) primary or (E) secondary dendrites. (F) Cypin overexpression increases the number of tertiary and higher order dendrites. Statistics were calculated by (A-B) two-way ANOVA followed by Tukey's multiple comparisons test or (C-F) one-way ANOVA followed by Dunnett's multiple comparison test ($n = 40$ for control, 42 for cypin and 34 for cypinΔPDZ).

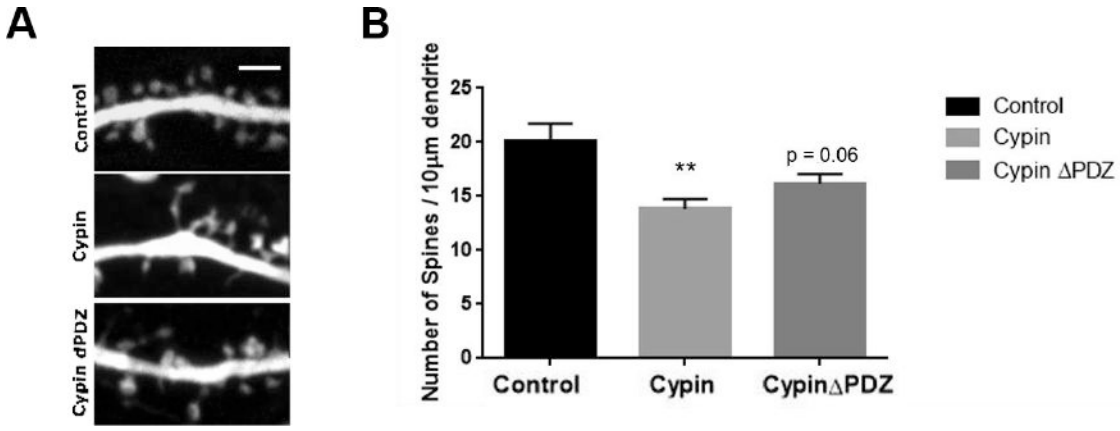

Figure 3. Cypin overexpression results in reduced spine density

(A) Representative images of dendritic segments from hippocampal neurons at DIV17. Scale bar = 2 μm. Images are of green fluorescent protein (GFP) channel as GFP is expressed throughout the entire neuron. (B) Overexpression of cypin results in a significant decrease in the density of dendritic spines. Overexpression of cypinΔPDZ results in a trend towards decreased spine density compared to control that is not statistically different from the spine density observed after cypin overexpression. Statistics calculated by one-way ANOVA followed by Tukey's multiple comparisons test (**$p < 0.01$). n=13-16 neurons per condition.

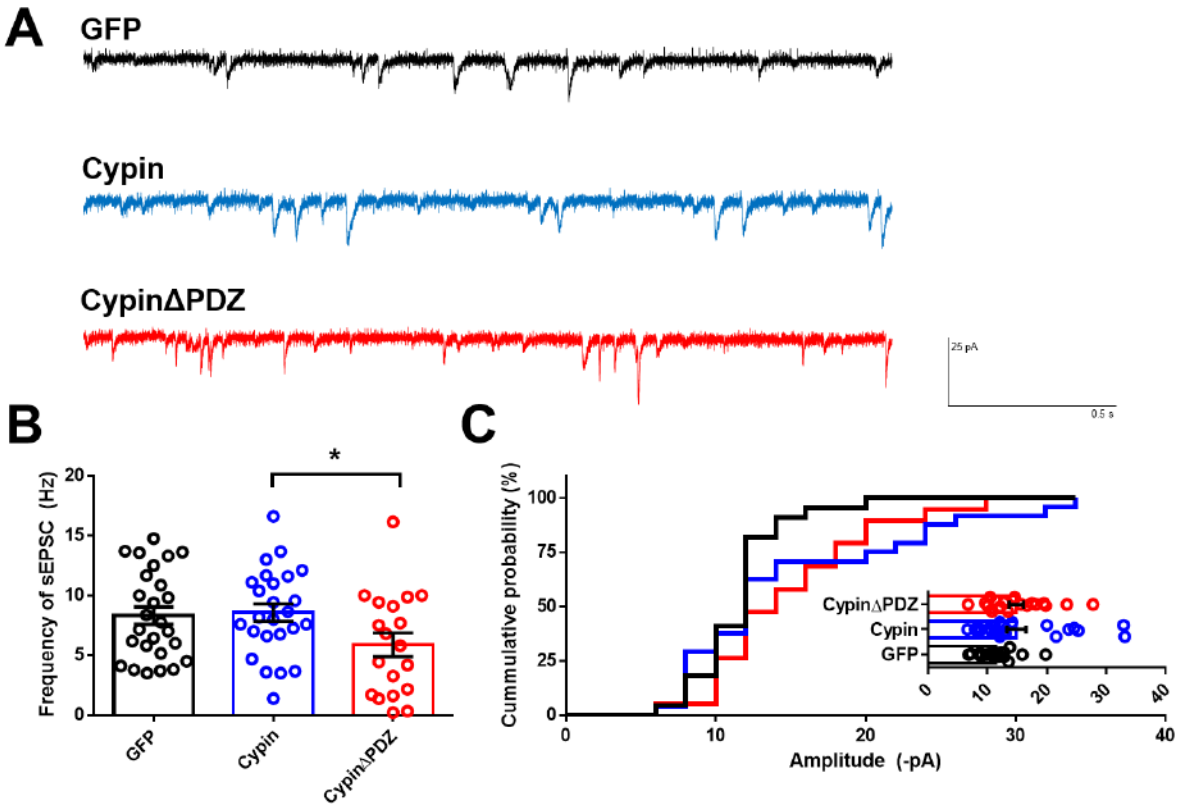

Figure 4. Whole cell patch clamp analysis shows that overexpression of cypin or cypinΔPDZ results in increased frequency of sEPSCs

(A) Representative traces of sEPSCs. (B) Overexpression of cypin does not change the frequency of sEPCs; however, overexpression of cypinΔPDZ decreases the frequency of sEPSCs when compared to cypin (*$p<0.05$). (C) The amplitude of sEPSCs remains unchanged after overexpression. Statistics calculated by one-way ANOVA followed by Tukey's multiple comparisons test (n = 26 for control, 25 for cypin and 19 for cypinΔPDZ).

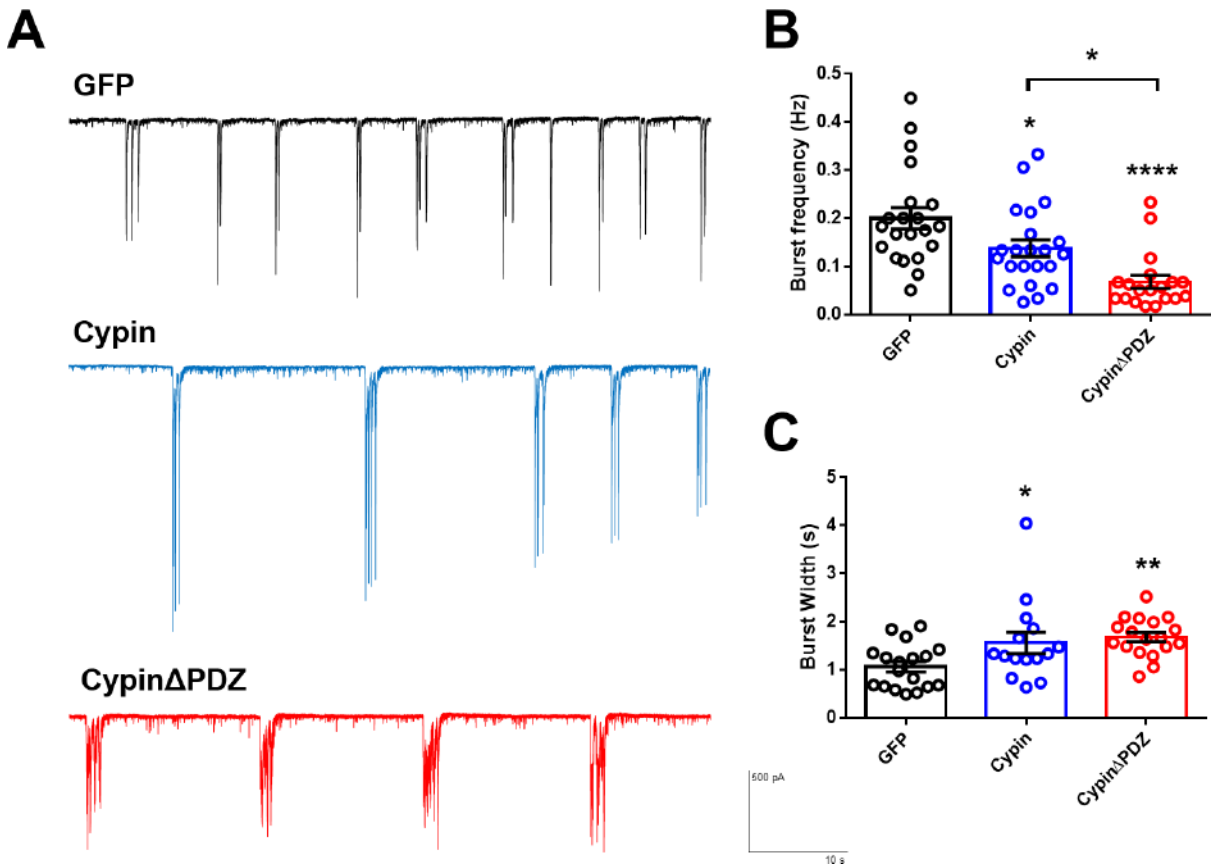

Figure 5. Whole cell patch clamp analysis shows that overexpression of cypin or cypinAPDZ results in decreased bursting frequency but increased duration

(A) Representative traces of sEPSCs and bursting events. (B) Overexpression of cypin or cypinΔPDZ decreases the frequency of bursting events when compared to GFP control (*p<0.05, ****p<0.001). (C) Burst width increased with overexpression of cypin or cypinΔPDZ. Statistics calculated by one-way ANOVA followed by Tukey's multiple comparisons test *(n* = 29 for control, 25 for cypin and 19 for cypinΔPDZ).

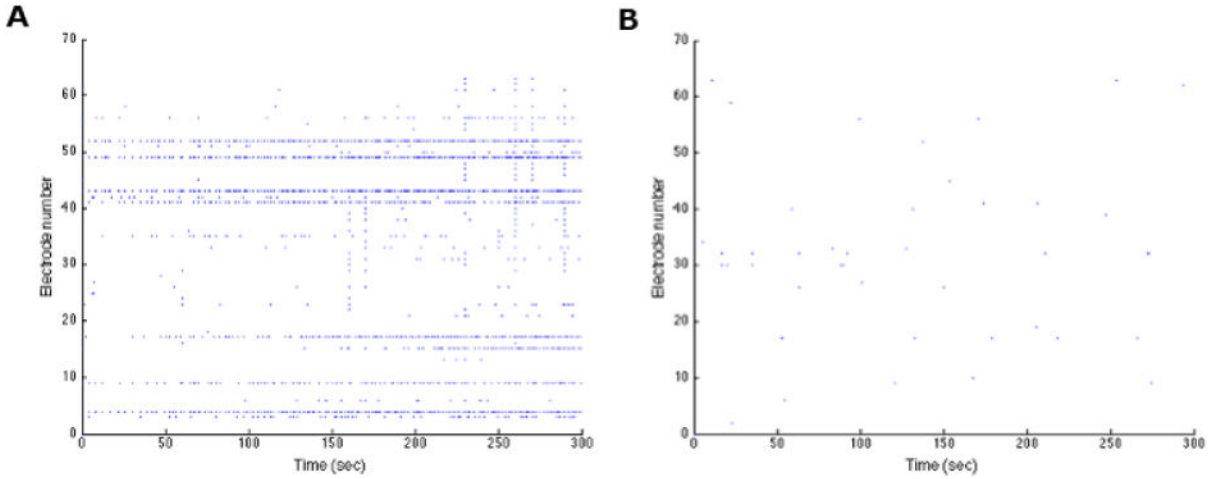

Figure 6. Culture activity decreases with synaptic blockade, suggesting that synaptic connections between neurons are driving firing properties

(A) The cultures show a high level of activity prior to exposure to synaptic blockers at DIV17. Each dot represents a recorded spike. (B) Treatment with synaptic blockers almost completely abolishes the spontaneous electrical activity of the networks.

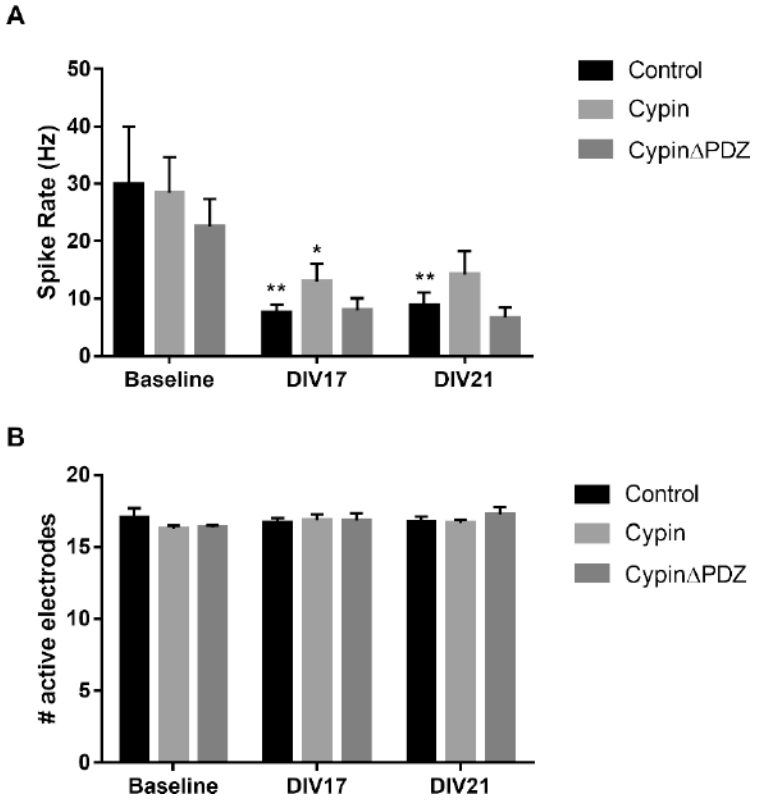

Figure 7. The effect of cypin overexpression on overall spike rate

(A) The rate of spiking activity decreases over time for control networks (**$p < 0.01$) with respect to their baseline. Networks that overexpress cypin show decreases in spike rate at DIV17 (*$p < 0.05$) and no decrease at DIV21 when compared to their baseline. The spike rate of networks that overexpress cypinΔPDZ demonstrate no decrease in spike rate on both DIV17 and 21. Statistics were calculated by two-way ANOVA followed by Tukey's multiple comparisons test vs. baseline for each condition ($n = 12$ for control, 14 for cypin and 11 for cypinΔPDZ). Extreme outliers were removed when identified by Grubb's test with $\alpha = 0.05$. (B) The number of active spiking electrodes is consistent between conditions. Active electrodes were defined when spike rate per electrode was ≥ the 75^{th} percentile of the distribution of spike rates for a particular culture. No statistical differences determined by two-way ANOVA followed by Tukey's multiple comparisons test ($n = 12$ for Control, 14 for Cypin and 11 for CypinΔPDZ).

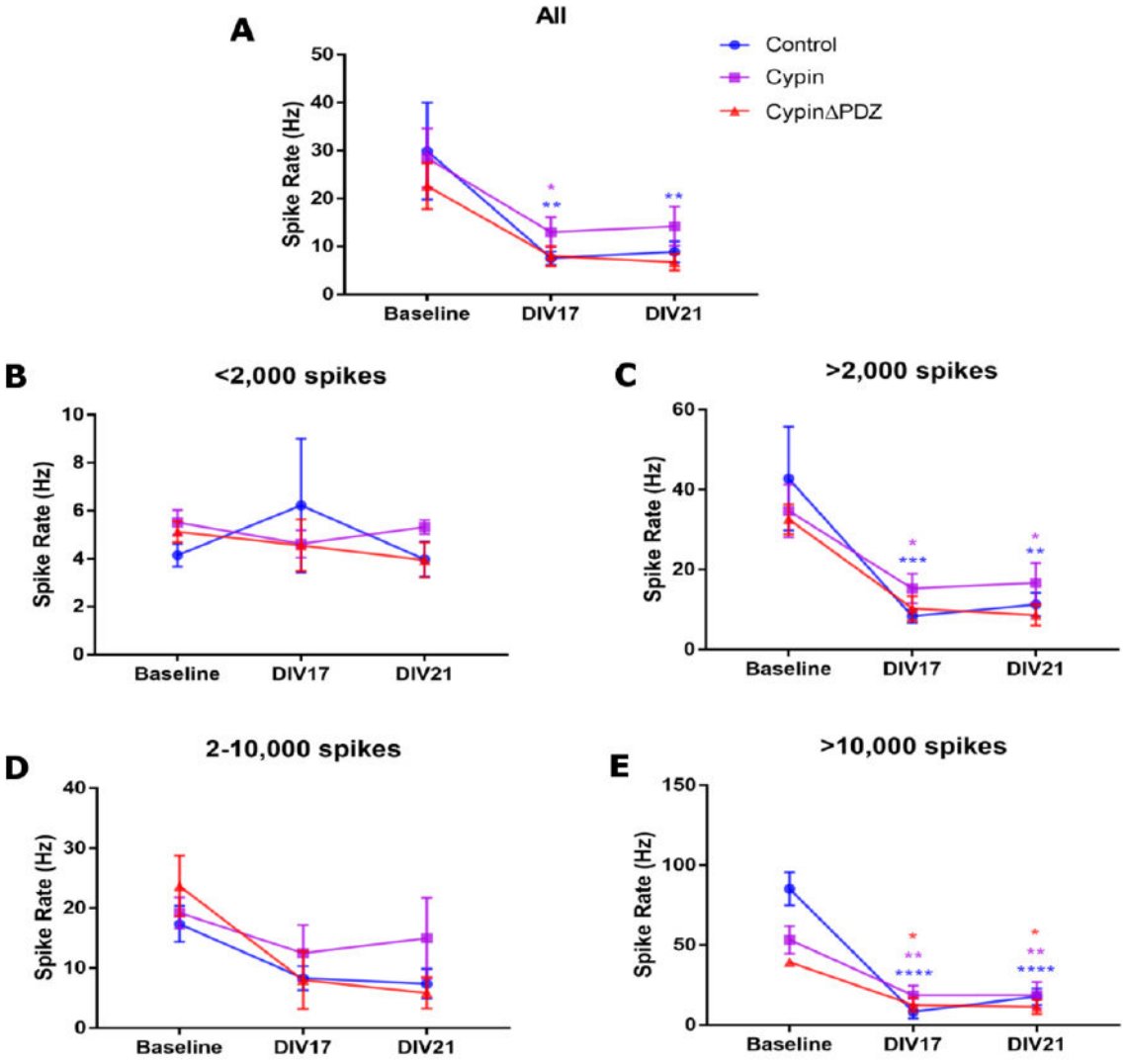

Figure 8. Baseline activity levels influence network activity over time

(A) Spike rates decrease by DIV17 and stabilize until DIV21 (n = 12 for Control, 14 for Cypin and 11 for CypinΔPDZ). (B) Cultures with low baselines do not exhibit changes in spike rate over time (n = 4 for Control, 3 for Cypin and 4 for CypinΔPDZ). (C) Low baseline cultures only contribute to the overall spike rate reduction for networks that overexpress cypin by DIV21 (n = 8 for Control, 11 for Cypin and 7 for CypinΔPDZ). (D) Network activity of cultures with intermediate baselines shows no change after transduction (n = 5 for Control, 6 for Cypin and 3 for CypinΔPDZ). (E) Spike rates decrease for all conditions in networks with high baselines (n = 3 for Control, 5 for Cypin and 4 for CypinΔPDZ). Statistics were calculated with respect to each group's baseline by two-way ANOVA followed by Tukey's multiple comparisons test (*p < 0.05, **p < 0.01, ***p < 0.001, ****p < 0.0001). Extreme outliers were removed when identified by Grubb's test with α = 0.05.

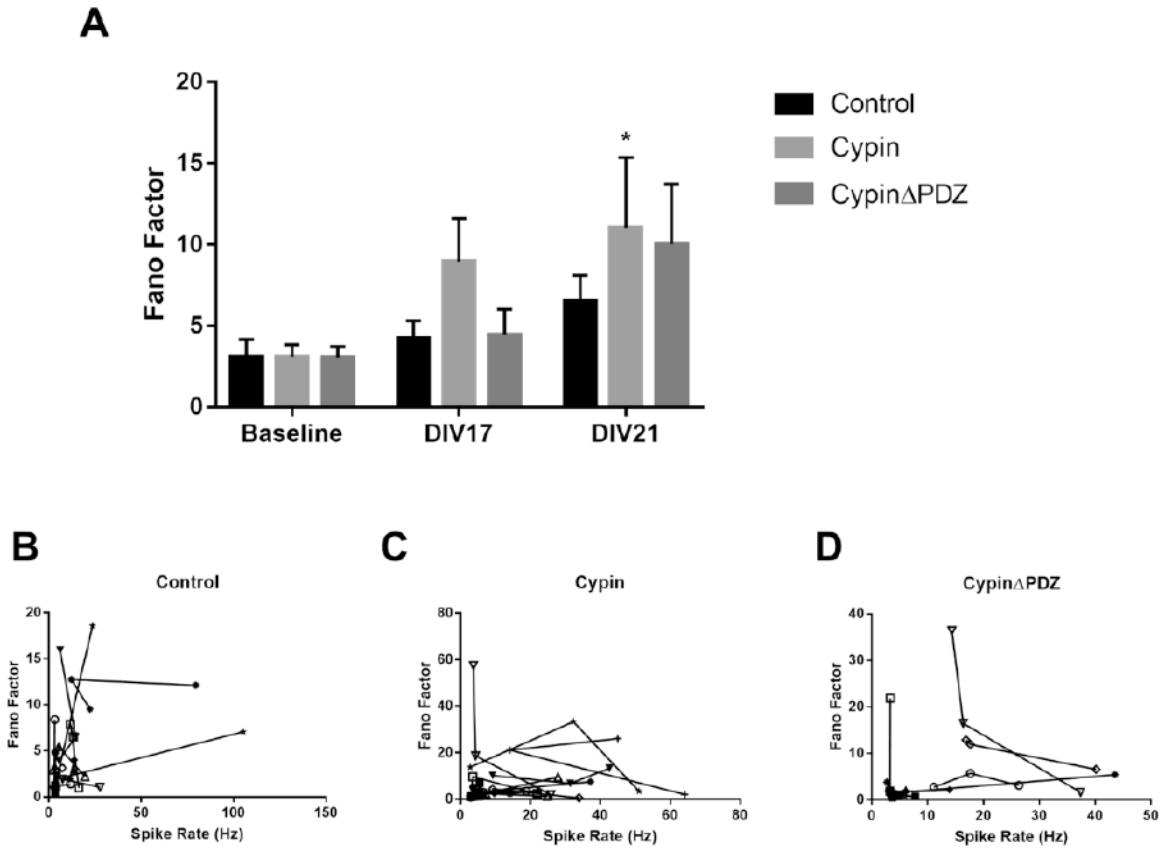

Figure 9. Spike count variability increases over time in networks that overexpress cypin

(A) Fano Factor increases after cypin overexpression (*p < 0.05), and this increase is dependent on PSD-95 binding. Statistics were calculated by two-way ANOVA followed by Tukey's multiple comparisons test (*n* = 12 for control, 14 for cypin and 11 for cypinΔPDZ). Extreme outliers were removed when identified by Grubb's test with α = 0.05. The Fano factor dependence on spike rate is highly variable. Networks overexpressing (B) GFP (Control; Spearman's rho = -0.1818 ± 0.2053; *n* = 12), (C) cypin (Spearman's rho = 0.07692 ± 0.2107; *n* = 14) and (D) cypinΔPDZ (Spearman's rho = 0.05556 ± 0.2693; *n* = 11) exhibit high trial-to-trial (recording session) variability in the relationship between spike count variability and spike rate.

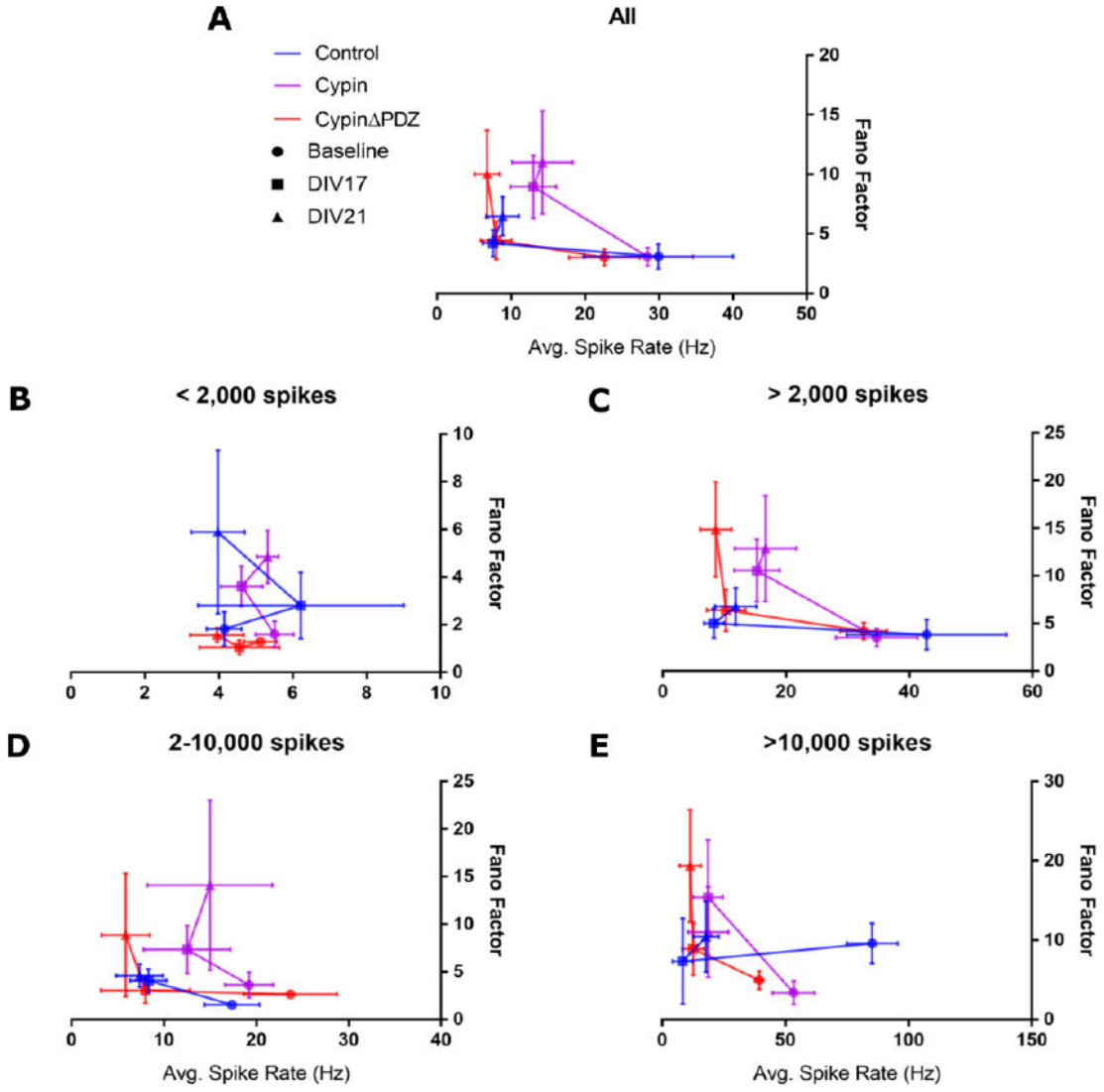

Figure 10. Dependence of Fano factor on baseline average spike rate

The average Fano factor is plotted versus the average spike rate for (A) all networks analyzed (n = 12 for control, 14 for cypin and 11 for cypinΔPDZ), (B) networks with low initial spike rates (n = 4 for control, 3 for cypin and 4 for cypinΔPDZ) (C) networks with intermediate and high initial spike rates (n = 8 for control, 11 for cypin and 7 for cypinΔPDZ) (D) networks with intermediate initial spike rates (n = 5 for control, 6 for cypin and 3 for cypinΔPDZ), and (E) networks with high initial spike rates (n = 3 for control, 5 for cypin and 4 for cypinΔPDZ). Because of the wide spread of data points along both axes, the mean ± s.e.m. is displayed. Each line has 3 data points: a circle (baseline), a square (DIV17), and a triangle (DIV21).

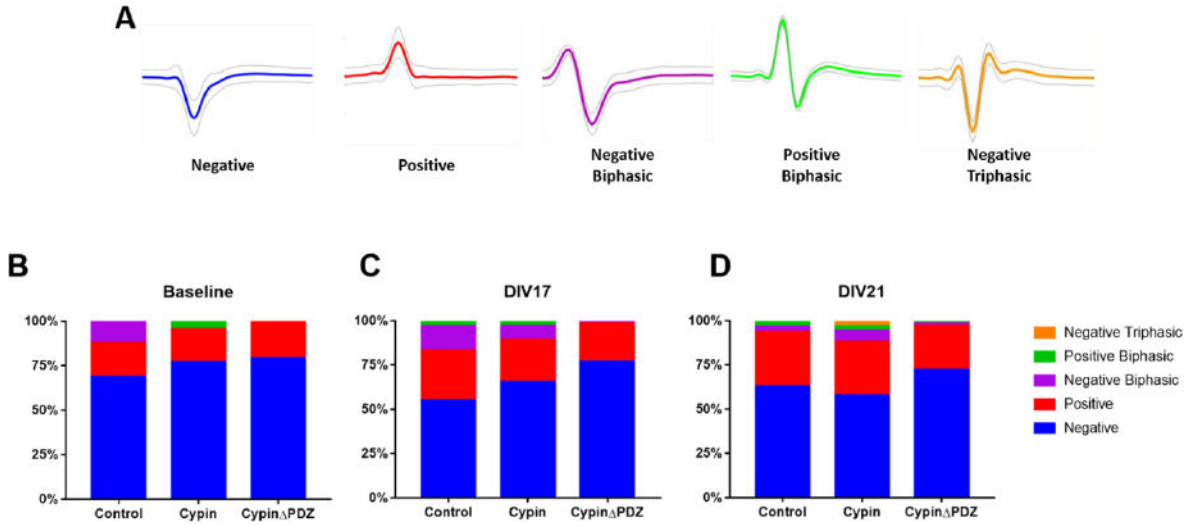

Figure 11. Categorization of the spike waveforms detected before and after transduction

(A) Representative average spike waveforms observed. Two monophasic, two biphasic, and one triphasic waveforms were detected. The distribution of waveforms of spontaneous spikes were determined at (B) baseline, (C) DIV17, and (D) DIV21. As expected from planar MEAs, the majority of waveforms detected are negative, but cypin overexpression leads to the detection of negative triphasic spikes, potentially related to an enhanced dendritic arbor.